Interstitial P_{CO_2} and pH, and their role as chemostimulants in the isolated respiratory network of neonatal rats

J. Voipio and K. Ballanyi*†

*Department of Biosciences, Division of Animal Physiology, PO Box 17, FIN-00014, University of Helsinki, Finland and *II Physiologisches Institut, Universität Göttingen, Humboldtallee 23, 37073 Göttingen, Germany*

1. CO_2–H^+-sensitive microelectrodes were used for simultaneous measurements of the partial pressure of CO_2 (P_{CO_2}) and extracellular pH (pH_o) in the ventral respiratory group (VRG) of the isolated brainstem–spinal cord of neonatal rats. Some of the data were analysed using diffusion equations.

2. With increasing recording depth within the boundaries of the VRG (300–600 μm below the tissue surface), P_{CO_2} increased from 77 to 95 mmHg and pH_o fell from 7·0 to 6·8 at steady state in standard saline equilibrated with 5% CO_2 and 95% O_2.

3. Elevating bath CO_2 from 5 to 10–12·5% produced a mean increase in P_{CO_2} of 18 mmHg, a fall in pH_o of 0·13 pH units, and a 50–250% increase in the frequency of respiration-related spinal (C2) nerve bursts. Similar effects on C2 activity and pH_o were observed upon lowering bath [HCO_3^-] from 25 to 10 mM, leading to a mean decrease in P_{CO_2} of 4·4 mmHg in the VRG.

4. Raising bath [HCO_3^-] to 50 mM produced a substantial frequency decrease, a rise in pH_o of 0·24 pH units and an elevation in P_{CO_2} of 9·3 mmHg. C2 activity was not profoundly affected upon doubling the CO_2–HCO_3^- content, leading to a mean increase in pH_o of 0·13 pH units and elevation of P_{CO_2} by 30 mmHg.

5. In a CO_2–HCO_3^--free, Hepes-buffered solution, P_{CO_2} decreased to 18 mmHg in the VRG and pH_o fell by 0·15 pH units with no major effect on rhythmic activity. Subsequent anoxic exposure for more than 15 min produced a further fall in P_{CO_2} to below 1 mmHg, a decrease in pH_o of 0·55 pH units, and blockade of respiration-related activity. In three out of the six preparations tested, C2 activity could be restored by reapplication of CO_2–HCO_3^- in the absence of O_2.

6. C2 activity persisted at a reduced frequency, even up to 30 min, during anoxia in the CO_2–HCO_3^--buffered saline, leading to an elevation in P_{CO_2} of 15 mmHg and a fall in pH_o of 0·18 pH units.

7. The diffusion coefficient of CO_2 in the tissue was found to be equal to that in saline. Two mean estimates for anoxic tissue of the function λ^2/α of tortuosity (λ) and extracellular volume fraction (α), affecting extracellular diffusion of bicarbonate, were 4·7 and 4·1. The mean rate of acid production by anoxic tissue was 1·1 mequiv l^{-1} min^{-1}.

8. The results suggest that extracellular H^+ is the primary stimulating factor in central chemosensitivity, which may often mask the less evident effects of CO_2. A model of diffusion of acid equivalents in brain tissue is proposed.

Central chemoreceptors play a crucial role in the control of breathing. Respiration is primarily stimulated by protons, but CO_2 is assumed to exert a direct response in addition to its indirect effect, caused by elevation of extracellular H^+ activity during hypercapnia (see Loeschcke, 1982; cf. Millhorn & Eldridge, 1986). In addition to uncertainty regarding the primary mechanism of central chemosensitivity, it is also questionable whether the chemoreceptive structures are restricted to the classical areas at the ventral surface of the medulla, originally described by the groups of Mitchell and Loeschcke (Loeschcke, 1982; Millhorn & Eldridge, 1986). For example, it has been reported that

† To whom correspondence should be addressed.

hypercapnia has a strong effect on the membrane potential and rhythmic activity of respiratory neurons of the VRG *in vivo* (St John & Wang, 1977) and *in vitro* (Kawai, Ballantyne, Mückenhoff & Scheid, 1996).

The latter study was carried out in the isolated brainstem–spinal cord of neonatal rats, in which the medullary respiratory network remains functionally intact (Suzue, 1984). This preparation is devoid of circulation and inputs from peripheral chemoreceptors, which modify the response of the respiratory network to disturbances of acid–base balance in the intact animal. Accordingly, this *in vitro* model is used in an increasing number of studies for the analysis of cellular mechanisms and localization of central chemosensitivity (e.g. Harada, Kuno & Wang, 1985; Okada, Mückenhoff & Scheid, 1993*b*; Völker, Ballanyi & Richter, 1995; Ballanyi, Völker & Richter, 1996; Kawai *et al.* 1996).

In order to discriminate between the effects of H^+ and CO_2 on chemosensitivity in this isolated medulla preparation, knowledge of the tissue levels of these chemostimulants is required. In addition, knowledge of the diffusion mechanisms by which metabolically produced acid leaves an *in vitro* brain tissue preparation is not well established. So far, only H^+-sensitive microelectrodes have been used for these purposes in the ventrolateral medulla of the brainstem–spinal cord preparation. In these studies, a rather steep tissue gradient for H^+ has been revealed (Brockhaus, Ballanyi, Smith & Richter, 1993; Okada, Mückenhoff, Holtermann, Acker & Scheid, 1993*a*; Völker *et al.* 1995). It was thought that metabolic lactate production, resulting in H^+ formation, might be the primary source of this pH gradient (Brockhaus *et al.* 1993; Völker *et al.* 1995; see also Chesler, 1990). A recent study using CO_2–H^+-sensitive microelectrodes suggests, however, that accumulation of interstitial CO_2 makes a major contribution to such acidosis in a brain slice preparation (Voipio & Kaila, 1993).

In the present study, we have used these electrodes to determine whether the pH_o gradient in the *en bloc* medulla is related to a gradient of P_{CO_2} (and $[HCO_3^-]_o$). It was a further aim to monitor P_{CO_2} and pH_o in the ventral respiratory group (VRG) during modifications of the CO_2–H^+–HCO_3^- content of the superfusion fluid. The present measurements allow, for the first time, a direct discrimination between the roles of H^+ and CO_2 in central chemosensitivity. Finally, we have measured effects on P_{CO_2}, pH_o and $[HCO_3^-]_o$ as well as their tissue profiles after blockade of aerobic CO_2 production by experimentally induced anoxia. A diffusion model is proposed to explain movements of acid equivalents in brain tissue. Estimates of the relevant diffusion parameters and of the metabolic rate in an anoxic preparation were calculated from the data using the proposed model. Some of the results have been published in abstract form (Voipio & Ballanyi, 1993; Kuwana, Ballanyi, Morawietz, Völker, Voipio & Richter, 1993).

METHODS

Preparation and solutions

The experiments were performed on brainstem–spinal cord preparations from 0- to 4-day-old rats. The animals were anaesthetized with ether, and the brainstem–spinal cord was isolated as reported previously (Brockhaus *et al.* 1993). The brainstem was transected at the pontomedullary junction, and the brainstem–spinal cord was pinned down in a Perspex chamber (volume, 5 ml) with the ventral side upwards. The tissue was superfused at a rate of 5 ml min^{-1} at 27 °C with the standard solution containing (mM): 118 NaCl, 3 KCl, 1·5 $CaCl_2$, 1 $MgCl_2$, 25 $NaHCO_3$, 1·2 NaH_2PO_4 and 30 D-glucose; equilibrated with nominally 5% CO_2 in O_2 (pH 7·4). Stainless-steel or Tygon (Norton Performance Plastics Corporation, Akron, OH, USA) tubing was used for gas supply and superfusion to avoid gas permeation through the tubing wall.

For analysis of the effects of chemostimulation, the standard solution was modified by changing two of the three acid–base parameters at a time (P_{CO_2}, $[HCO_3^-]$, pH) while keeping the third one constant. Changing the gas to one containing nominally 10% (or 12·5%) CO_2 in O_2, as well as decreasing the $[HCO_3^-]$ to 10 mM (equimolar substitution with Cl^-), gave a solution with a pH of 7·1 (or 7·0) and 7·0, respectively. An increase in solution pH to 7·7 was achieved by increasing the $[HCO_3^-]$ to 50 mM. In some experiments, $[HCO_3^-]$ was increased to 50 mM (or 63 mM) by equimolar substitution for Cl^- and the solutions were equilibrated with nominally 10% (or 12·5%) CO_2 in O_2, respectively, thereby maintaining a constant pH of 7·4. The nominally CO_2–HCO_3^--free Hepes-buffered saline was equilibrated with 100% O_2 and contained (mM): 118 NaCl, 3 KCl, 1·5 $CaCl_2$, 1 $MgCl_2$, 25 Hepes and 30 D-glucose (pH adjusted to 7·4 with NaOH). Hypoxic conditions (partial pressure of oxygen (P_{O_2}) < 25 mmHg; Brockhaus *et al.* 1993; Völker *et al.* 1995) were produced by gassing of the standard or Hepes-buffered solutions with 5% CO_2 in N_2 or with 100% N_2, respectively. In some experiments, benzolamide (an impermeant inhibitor of carbonic anhydrase; 50 μM; donated by Lederle Laboratories, American Cyanamide Company) was added from a 10 mM stock solution made in 10 mM NaOH.

The gas mixtures mentioned above were compared with a reference gas with an accurate CO_2 content by applying the CO_2 microelectrode technique (see below) and pH measurement in well-equilibrated solutions. Deviations from nominal CO_2 levels were taken into account and, throughout the paper, the CO_2 content of superfusion solutions expressed as the partial pressure of CO_2 (P_{CO_2}) correspond to the corrected CO_2 levels. The effect of saturated water vapour at 27 °C was taken into account by assuming 100% CO_2 to be equal to 734 mmHg P_{CO_2}.

CO_2–H^+-sensitive microelectrodes

Double-barrelled CO_2–H^+-sensitive microelectrodes were made as described previously using the PVC/BBPA membrane solution (Voipio & Kaila, 1993) and with an increased concentration of carbonic anhydrase in the CO_2-sensitive barrel (4 mg ml^{-1}; Voipio, Pasternack & MacLeod, 1994). The membrane column in the CO_2-sensitive barrel was made longer (10–45 μm) to improve its mechanical strength for deep impalements into the tissue (see below). Electrodes selected for the experiments had a 90% response time (t_{90}) of 4–20 s upon a step change in P_{CO_2} from 41 to 76 mmHg. Triple-barrelled CO_2–H^+-microelectrodes were made using special triple-barrelled tubing (3GC120SF; Clark Electromedical Instruments, Pangbourne, Reading, UK; for details, see Voipio *et al.* 1994), which consists of one filamented and two non-filamented capillaries fused together. The filamented barrel, which

was not silanized, was filled with 150 mM NaCl and acted as a reference electrode for recording extracellular potential. Since extracellular potential changes recorded in the tissue always remained within a range of a few hundred microvolts, the pH barrel signal was used (instead of the differential pH signal) for pH_o in experiments with double-barrelled CO_2–H^+-sensitive microelectrodes.

All CO_2–H^+-sensitive microelectrodes were calibrated in mixtures of 200 mM NaCl and 200 mM $NaHCO_3$ before and, in most cases, after each experiment using at least two physiologically relevant P_{CO_2} levels (41 and 76 mmHg) at a constant pH, and using two pH levels (7·4 and 7·7) at a constant P_{CO_2} value of 41 mmHg. The slope of the pH response, as well as that of the logarithmic P_{CO_2} response, was calculated for each individual electrode. The latter slope (m_{CO_2}) was obtained by using the equation:

$$V_{CO_2,diff} = V_0 + m_{CO_2} \log P_{CO_2}, \quad (1)$$

where V_0 is a constant and the CO_2-sensitive signal, $V_{CO_2,diff}$, is obtained by subtracting the CO_2 barrel signal from the pH barrel signal (see Voipio & Kaila, 1993).

At P_{CO_2} levels lower than 13·5 mmHg, the electrodes were calibrated using a Hepes-buffered NaCl solution equilibrated with air, assuming a CO_2 content of 0·035% or 0·26 mmHg. The upper trace in Fig. 1*A* shows a specimen recording of the response of the $V_{CO_2,diff}$ signal to three calibration solutions. The lower trace shows the measured data on a linear P_{CO_2} scale and was obtained by first solving V_0 and m_{CO_2} as described above and then, using eqn (1), obtaining P_{CO_2}. Note that the response time of the electrode or the kinetics of a P_{CO_2} change in a preparation cannot be seen directly from the electrode signal, $V_{CO_2,diff}$, especially at low P_{CO_2} levels. In order to emphasize this, a vertical dashed line has been drawn in Fig. 1*A* to indicate the t_{90} of the measured P_{CO_2} ($P_{CO_2,meas}$) upon a change in P_{CO_2} from 41 to 0·26 mmHg. In Fig. 1*B*, the mean amplitudes of $V_{CO_2,diff}$ responses (± S.D., 55 electrodes) have been plotted against the P_{CO_2} of the calibration solutions ($P_{CO_2,cal}$). Fitting a line to the mean values at 15, 41 and 76 mmHg gives a slope of

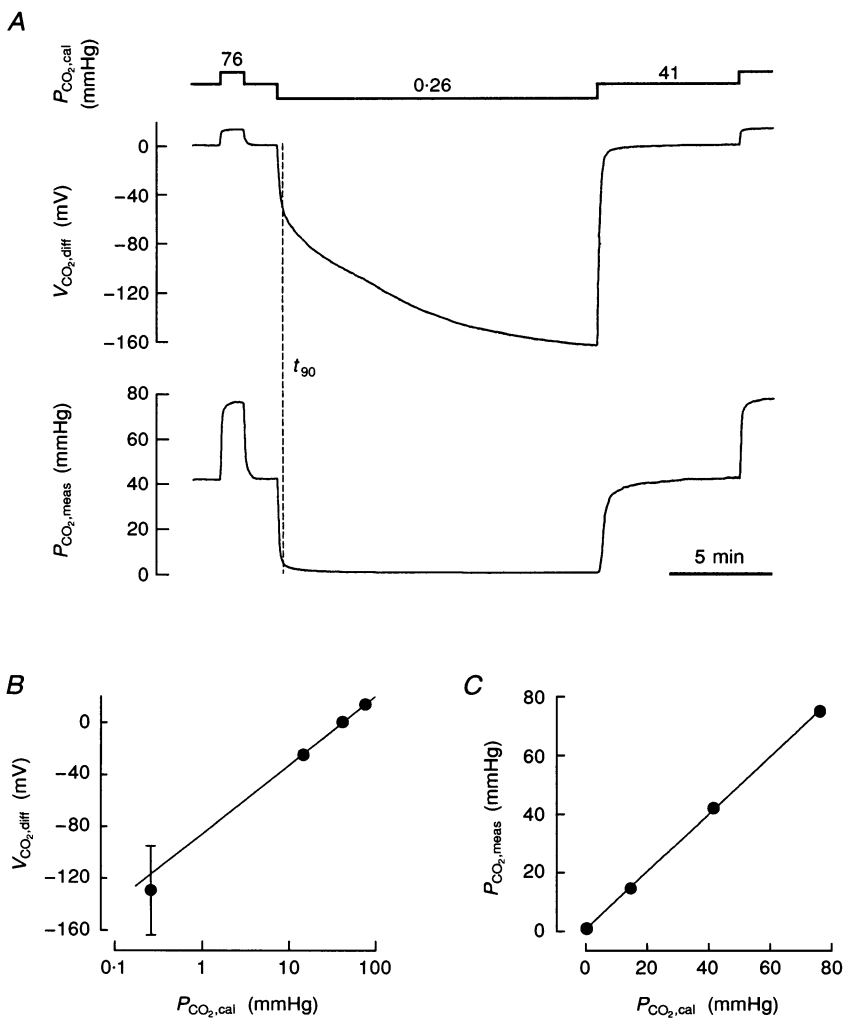

Figure 1. Calibration of the CO_2–H^+-sensitive microelectrodes

A, the logarithmic nature of the CO_2-sensitive primary signal ($V_{CO_2,diff}$) shows an apparently exaggerated response at low levels of P_{CO_2} in the calibration solution ($P_{CO_2,cal}$). The linearized measured signal ($P_{CO_2,meas}$) falls rapidly upon a change in $P_{CO_2,cal}$ to 0·26 mmHg, as emphasized by the dashed line indicating the moment of reaching 90% of the response (t_{90}). *B*, mean amplitudes of $V_{CO_2,diff}$ (± S.D., 55 electrodes) plotted against $P_{CO_2,cal}$. The potential recorded at $P_{CO_2,cal}$ of 41 mmHg has been assigned zero. The straight line was fitted using values at 15, 41 and 76 mmHg. *C*, mean $P_{CO_2,meas}$ values from *B* plotted against $P_{CO_2,cal}$. Note the wide working range of the electrodes.

53 mV for a tenfold change in P_{CO_2}. The excellent correlation between $P_{CO_2,meas}$ and $P_{CO_2,cal}$ throughout the whole P_{CO_2} range is demonstrated by the plot in Fig. 1*C*, which was obtained by linearizing the mean values of $V_{CO_2,diff}$ shown in Fig. 1*B*.

Monitoring of tissue pH, P_{CO_2} and respiratory activity

The surface of the tissue was detected during slow advance of the triple-barrelled CO_2–H^+-sensitive microelectrodes as a transient shift in the signal of the reference barrel (V_{ref}). In the experiments with double-barrelled microelectrodes, the position of the tissue surface was determined under microscopic control by observing tissue movements in response to lateral displacements (±20–30 μm) during slow advance of the microelectrode. For the analysis of changes in P_{CO_2} and pH_o, electrodes were positioned either 500–700 μm above the ventral surface, or at a depth of 400–500 μm, which corresponds to the centre of the cell column representing the VRG (Brockhaus *et al.* 1993).

Inspiration-related discharges were recorded extracellularly with suction electrodes applied at proximal ends of ventral roots of spinal (C2) nerves. The signals of axons of active respiratory motoneurons were amplified, bandpass filtered (0·5–1·5 kHz), rectified and integrated before displaying and storage.

Data storage and analysis

Nerve activities as well as microelectrode signals were digitized and recorded on magnetic tape. During the experiments, signals were also displayed on a chart recorder. All P_{CO_2} traces shown have been obtained by linearizing the recorded $V_{CO_2,diff}$ signals using Asystant+ (Macmillan Software Company, New York) software. Sigmaplot (Jandel Corporation, San Rafael, CA, USA) and Designer (Micrografx, Inc., Richardson, TX, USA) software packages were used for statistical analysis and preparation of the figures. All values in this study are means ± S.D.

Indirect recording of bicarbonate concentration

$[HCO_3^-]$ can be calculated from P_{CO_2} and pH if the CO_2 hydration–dehydration reaction is under equilibrium. Using benzolamide, evidence was obtained for the presence of functionally active extracellular carbonic anhydrase in the present preparation (see Results). Since, as well, the changes in pH_o and tissue P_{CO_2} were relatively slow, it was considered justified to convert the primary signals into a continuous recording of $[HCO_3^-]_o$. The calculation was done using Asystant+ software with the solubility (S_{CO_2}) and the first dissociation constant (pK_1') of CO_2 equal to 0·04 mM $mmHg^{-1}$ and 6·17, respectively, in the Henderson–Hasselbalch equation:

$$[HCO_3^-] = S_{CO_2} P_{CO_2} 10^{pH-pK_1'}. \quad (2)$$

RESULTS

Tissue profiles of P_{CO_2}, pH_o and $[HCO_3^-]_o$

Previous work has demonstrated a marked fall in pH_o and also in the partial pressure of O_2 with increasing tissue depth in the brainstem–spinal cord (Fig. 2*A*) maintained in the standard CO_2–HCO_3^--containing solution (Brockhaus *et al.* 1993; Okada *et al.* 1993*a*). The relation of these gradients, which indicate a high rate of metabolic activity (Ballanyi *et al.* 1996), to an assumed gradient of P_{CO_2} was studied in an initial series of experiments. Figure 2*C* shows an experiment in which tissue profiles of pH_o, P_{CO_2} and extracellular potential were measured simultaneously along the electrode track of Fig. 2*B* with a triple-barrelled CO_2–H^+ microelectrode. Advancing the electrode in 100 μm steps from the bulk solution into the preparation, indeed, revealed that the pH_o gradient is associated with a prominent gradient of P_{CO_2}. However, as indicated by the signal of the reference barrel (V_{ref}) of the triple-barrelled microelectrode, these tissue gradients were not accompanied by any measurable gradient of extracellular potential.

Application of the membrane-impermeant carbonic anhydrase inhibitor benzolamide (50 μM) produced a sustained fall in pH_o in the VRG, which developed at a rate of about 0·005 pH units min^{-1} (not illustrated), thereby indicating the presence of extracellular carbonic anhydrase in a manner similar to that seen in rat hippocampal slices (Kaila, Paalasmaa, Taira & Voipio, 1992; Voipio, Paalasmaa, Taira & Kaila, 1995). It was therefore considered justified to assume equilibrium of the CO_2 hydration–dehydration reaction (cf. Maren, 1984) in the extracellular space and to calculate $[HCO_3^-]_o$ (see Methods), which also showed a tissue profile mirroring those of pH_o and P_{CO_2}.

Figure 2*D* summarizes the results of similar recordings from fourteen preparations with either double-barrelled or triple-barrelled microelectrodes. The peak values of P_{CO_2}, pH_o and $[HCO_3^-]_o$ were 106·1 ± 7·6 mmHg, 6·65 ± 0·10 pH units and 12·9 ± 2·0 mM, respectively, and they were observed at a depth of about 1100 μm. At greater depths, the electrode tip passed the core of the preparation, which was seen as a decline of P_{CO_2} and an increase of pH_o and $[HCO_3^-]_o$. In the region of the VRG (see shaded area in Fig. 2*D*), which is located 300–600 μm below the tissue surface in the ventrolateral reticular formation near the nucleus ambiguus (Fig. 2*B*; see also Brockhaus *et al.* 1993), mean P_{CO_2} increased from 77·3 to 95·1 mmHg, whereas pH_o fell from 6·98 to 6·79 pH units and $[HCO_3^-]_o$ fell from 20·1 to 16·1 mM. Omitting NaH_2PO_4 from the standard saline did not have a noticeable effect on pH_o or V_{ref} in the VRG (not shown). The gradients of P_{CO_2} and pH in the superfusate close to the preparation indicate an unstirred layer (cf. Gutknecht & Tosteson, 1973).

Effects of changing bath pH, P_{CO_2} and bicarbonate

In order to test the effects on respiration-related C2 activity of experimentally induced changes in pH_o, P_{CO_2} and $[HCO_3^-]_o$ in the VRG, the preparations were exposed to solutions with altered CO_2–H^+–HCO_3^- content.

Extracellular acidosis

Figure 3 shows an experiment where tissue acidosis was induced first by superfusing the preparation with the 10 mM HCO_3^-, pH 7·0 solution (constant P_{CO_2} of 41 mmHg) and, after washout, by shifting to a solution with a P_{CO_2} of 92 mmHg and a pH of 7·0 (constant HCO_3^- content of 25 mM). The fall in pH_o induced by reducing $[HCO_3^-]$ was paralleled by a fall in both tissue P_{CO_2} and $[HCO_3^-]_o$ in the

VRG, whereas the hypercapnia-induced acidification with a similar amplitude was coupled to an increase in tissue P_{CO_2} of more than 20 mmHg with little change in $[HCO_3^-]_o$. It is important to note that, despite opposite changes in tissue P_{CO_2}, both types of acidification were associated with a distinct augmentation of respiratory activity, as shown by an increase in the frequency of inspiration-related C2 bursts.

The mean decrease in pH_o upon superfusing with the constant-HCO_3^- solution having a high P_{CO_2} of 76 or 92 mmHg was $0{\cdot}13 \pm 0{\cdot}03$ pH units, while tissue P_{CO_2} increased by $17{\cdot}8 \pm 8{\cdot}2$ mmHg ($n = 9$). In eight out of the nine preparations, these changes in P_{CO_2} and pH_o were accompanied by an increase in the frequency of respiratory activity of between 50 and 250%, whereas the amplitude or the duration of individual inspiratory bursts remained unchanged. In one preparation, this type of solution did not affect respiratory frequency, despite comparable changes of P_{CO_2} and pH_o in the VRG. A similar frequency increase and a fall in pH_o of $0{\cdot}19 \pm 0{\cdot}07$ pH units were recorded from the seven preparations tested in the more acidic (pH 7·0) solution containing 10 mM HCO_3^-. Under these conditions, tissue P_{CO_2} decreased by $4{\cdot}4 \pm 5{\cdot}3$ mmHg. The slow time course of the pH_o and P_{CO_2} changes has its origin within the tissue, since the solution exchange in the experimental chamber occurred at a much faster rate (see calibration on the right in Fig. 3).

Extracellular alkalosis

Increasing the pH of the standard saline to 7·7 by elevation of the bicarbonate concentration to 50 mM led to a prominent rise of pH_o in the VRG by $0{\cdot}24 \pm 0{\cdot}06$ pH units ($n = 4$) and of P_{CO_2} by $9{\cdot}3 \pm 6{\cdot}1$ mmHg. As shown in Fig. 4, the tissue alkalosis was coupled to substantial depression of

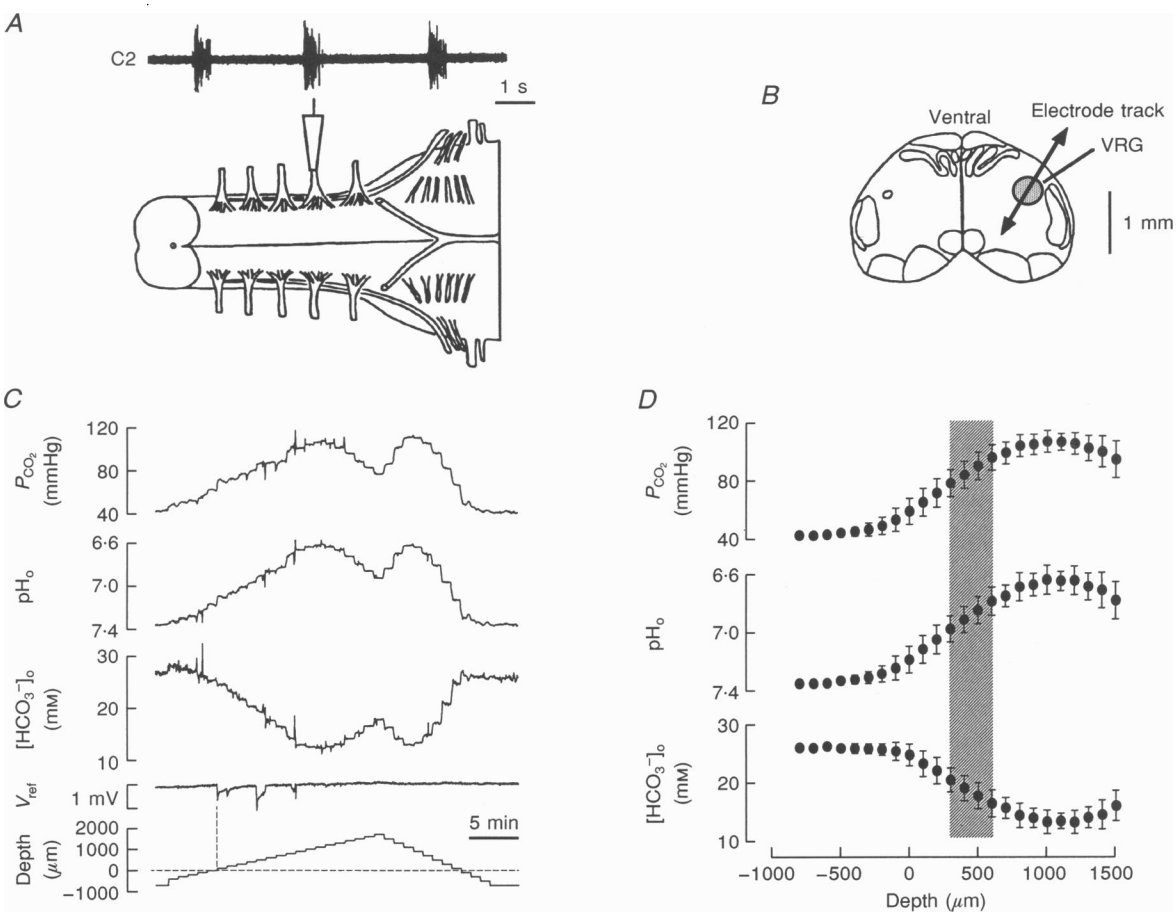

Figure 2. Tissue profiles of P_{CO_2}, pH_o and $[HCO_3^-]_o$

A, schematic drawing of the *in vitro* brainstem–spinal cord preparation with a suction electrode attached for extracellular recording of C2 activity (specimen recording shown on an expanded time scale). *B*, cross-section of the preparation showing location of the VRG (shaded area) and the electrode track used in *C*. *C*, profiles of P_{CO_2}, pH_o, $[HCO_3^-]_o$ and potential (V_{ref}), as measured with a triple-barrelled CO_2–H^+-sensitive microelectrode during superfusion with standard saline. The electrode was moved along the track shown in *B* in steps of 100 or 200 μm from bulk solution deep into the tissue and back, as indicated with respect to tissue surface by the nominal depth trace. The first negative deflection of V_{ref} indicates contact with tissue surface (vertical dashed line). *D*, mean values of P_{CO_2}, pH_o and $[HCO_3^-]_o$ (± S.D., 14 preparations) at different depths. The shaded area indicates the region of the VRG.

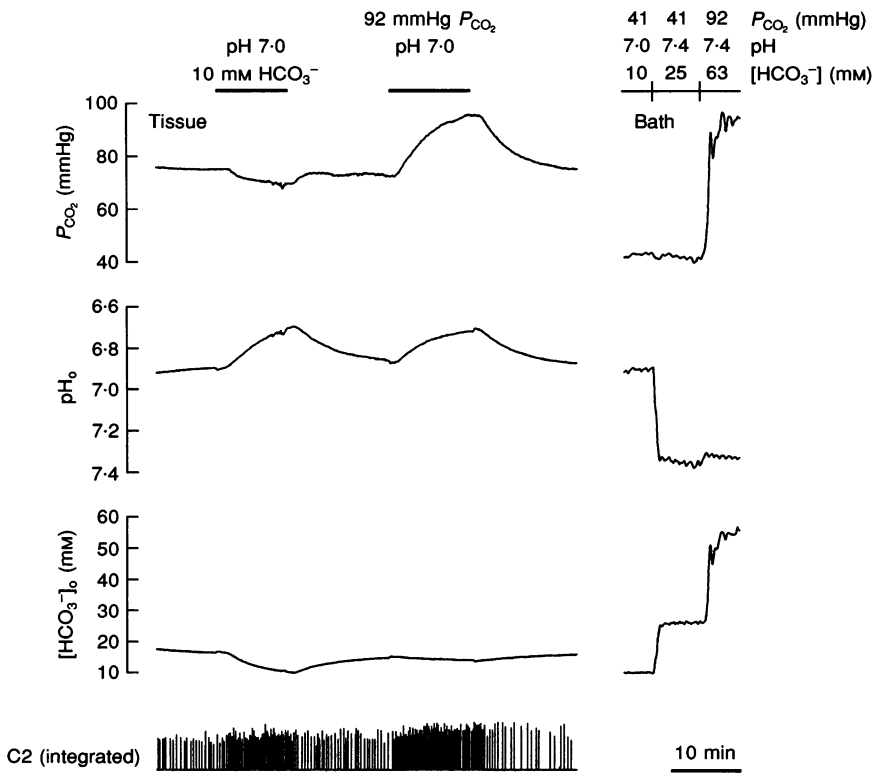

Figure 3. Effects of extracellular acidification

Extracellular acidification in the VRG gives rise to an increase in the frequency of C2 bursts (seen as single vertical spikes due to the compressed time scale). Note opposite changes in P_{CO_2} in the VRG upon superfusion with the two solutions of pH 7·0 having low $[HCO_3^-]$ (constant P_{CO_2} of 41 mmHg) or high P_{CO_2} (constant $[HCO_3^-]$ of 25 mM). Shown on the right is a calibration, which was made in the bath after withdrawing the electrode from the preparation by first changing pH from 7·0 to 7·4 at a constant P_{CO_2} and then changing P_{CO_2} from 41 to 92 mmHg at a constant pH.

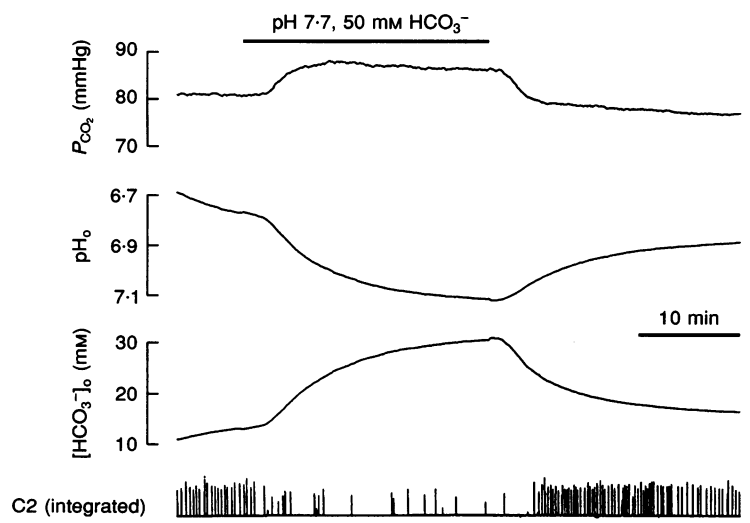

Figure 4. Effects of extracellular alkalosis

An increase in pH_o in the VRG is associated with substantial reduction in the frequency of C2 bursts in spite of a simultaneous increase in tissue P_{CO_2}.

respiratory activity that could lead to a reduction of the frequency of respiratory bursts to less than 1 min^{-1}.

In contrast to these results suggesting a simple relationship between pH_o and respiratory activity, an extracellular alkalosis of 0·13 ± 0·10 pH units, associated with hypercapnia at a constant solution pH, did not affect the steady-state frequency or pattern of inspiratory bursts in six out of the fifteen preparations (Fig. 5*A*). This alkalosis was elicited by increasing $[HCO_3^-]$ to 50 mM and P_{CO_2} to 76 mmHg, and it was accompanied by a rise in P_{CO_2} in the VRG of 29·9 ± 15·0 mmHg. In the remaining nine cases, variations in the steady-state respiratory cycle length up to −50 to +100% (mean, −14%) of the control value were observed (not illustrated). A temporary increase (mean of peak, 65%) in the frequency was evident in five of the fifteen preparations during the rising phase of P_{CO_2} (not illustrated).

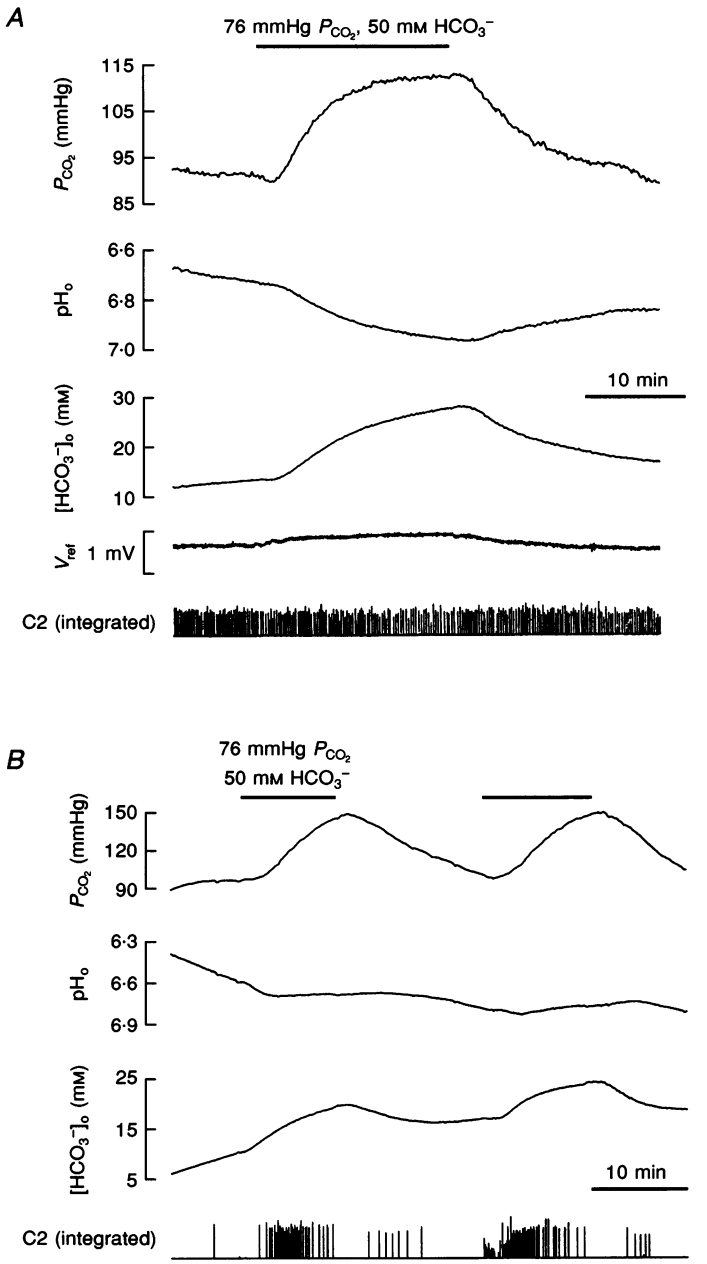

Figure 5. Effects of hypercapnia at a constant solution pH

A, moderate rise in pH_o paralleled by a large increase in P_{CO_2}, seen in the VRG upon superfusion with a hypercapnic solution at a constant solution pH, does not perturb C2 activity. *B*, similar experiment shows chemostimulation associated with an increase in tissue P_{CO_2} in a preparation in which rhythmic activity ceased during the course of a long-lasting experiment.

The two solutions with 50 mM bicarbonate induced a pronounced rise in $[HCO_3^-]_o$ of 14·7 ± 4·5 mM (alkaline solution) and 12·7 ± 6·7 mM (hypercapnic solution), i.e. in this respect both these solutions had a similar effect.

In line with the temporary stimulating effect of CO_2, we found reactivation of rhythmic activity in three preparations, in which C2 bursts spontaneously disappeared after recording sessions of several hours (Fig. 5*B*). The evident coincidence of the early phase of P_{CO_2} rise and of frequent bursts in C2 seen in Fig. 5*B* suggests that the stimulating factor is, at least partly, the rate of rise of P_{CO_2}. This suggests that intracellular acidification might be involved in the underlying mechanisms.

CO_2-free solutions

Effects of the nominally CO_2–HCO_3^--free Hepes-buffered saline were analysed in a different series of experiments. Superfusion of this solution led to a rapid depletion of CO_2 in the experimental chamber, which was accompanied by a slow and apparently exponential decrease in P_{CO_2} in the VRG, attaining a stable level of 17·6 ± 6·4 mmHg ($n = 9$) in 30–45 min (Fig. 6*A* and *B*). Under these conditions, pH_o fell by 0·15 ± 0·06 pH units ($n = 9$; Fig. 6*B*) and, at steady state, $[HCO_3^-]_o$ was still 2·6 ± 1·5 mM, which can be accounted for by hydration of metabolically produced CO_2. After recovery from initial perturbances induced by the introduction of this solution, the pattern of inspiratory

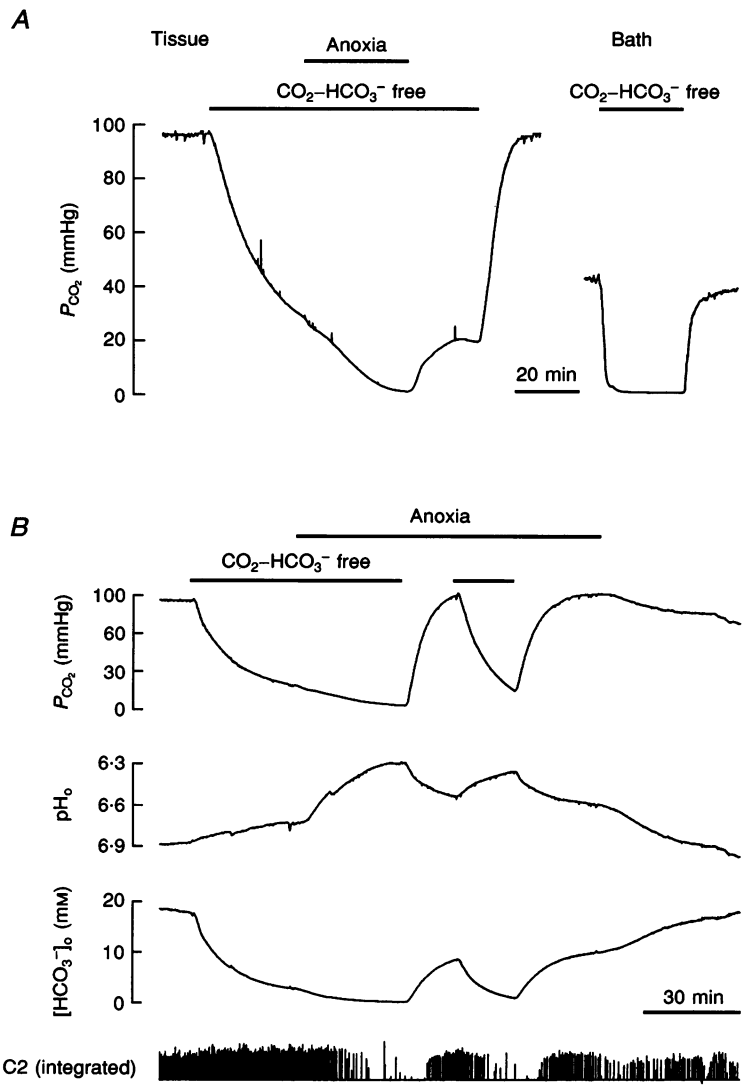

Figure 6. Effects of solutions free of CO_2 and/or O_2

A, switching to the nominally CO_2–HCO_3^--free oxygenated saline causes a substantial fall in P_{CO_2} in the VRG. However, a complete depletion of tissue CO_2 is seen only upon anoxia in the absence of CO_2–HCO_3^-. Calibration of the electrode shown on the right was made 700 μm above the preparation and it indicates a rapid solution change in the experimental bath. *B*, anoxia induced in the nominal absence of CO_2–HCO_3^- gives rise to a pronounced acidification paralleled by depletion of both CO_2 and HCO_3^- from the tissue. Note the reproducible recovery of C2 activity upon reapplication of CO_2–HCO_3^- during prolonged anoxia.

bursts was almost identical to that in the standard saline and the frequency of respiratory rhythm changed by ±30% at most (mean, +1%).

These results support the idea that extracellular H^+ ions have a major influence on respiration-like activity *in vitro*. However, it appears that CO_2 plays only a minor role as a chemostimulus at steady state (Loeschcke, 1982). In addition, it may cause temporary effects associated with changes in P_{CO_2}.

Effects of anoxia

Anoxia during hypocapnia

After reaching steady state following withdrawal of CO_2–HCO_3^-, anoxia of the entire preparation (cf. Brockhaus *et al.* 1993; Völker *et al.* 1995) was induced by switching to the Hepes-buffered solution equilibrated with 100% N_2 instead of 100% O_2. This induced a further fall in P_{CO_2} to levels below 1·0 mmHg at steady state in the VRG. Subsequent exposure to 100% O_2 led to an increase in P_{CO_2} to approximately the pre-anoxic value (Fig. 6*A*). The difference between tissue P_{CO_2} levels during anoxia and in the oxygenated, Hepes-buffered solution reflects CO_2 in the VRG, which is generated by aerobic metabolism.

As shown in Fig. 6*B*, the anoxia-induced depletion of CO_2 from the tissue was paralleled by a further fall in pH_o of 0·55 ± 0·29 pH units ($n = 9$) and a decline in extracellular bicarbonate to submillimolar levels. These effects were coupled to a reduction in the frequency of respiratory

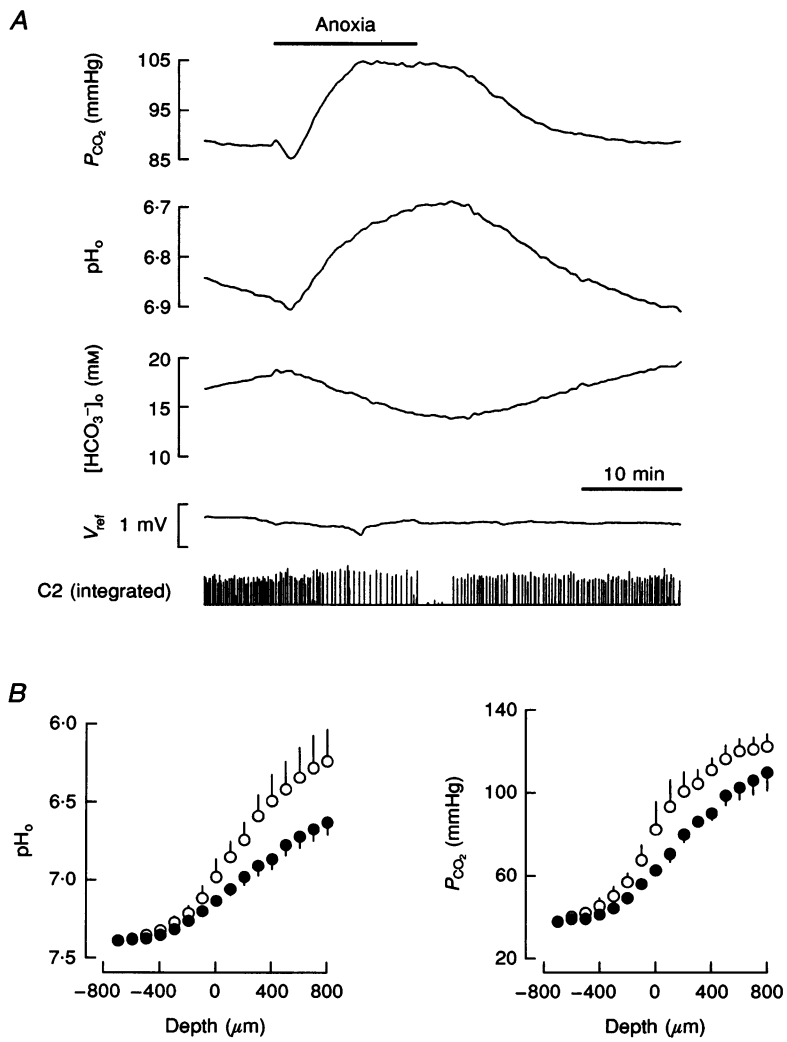

Figure 7. Anoxia at constant solution P_{CO_2}

A, blocking aerobic metabolism in the CO_2–HCO_3^--containing solution by induction of anoxia leads to a rise in P_{CO_2} and a fall in both pH_o and $[HCO_3^-]_o$ in the VRG, and a progressive decline in the frequency of C2 bursts. The complete block of C2 activity coincides with reapplication of O_2. Note that there is little change in V_{ref} during anoxia. *B*, steady-state profiles of pH_o and P_{CO_2} (mean ± S.D., 5 preparations) in the oxygenated standard solution (●) and during anoxia induced by withdrawal of O_2 (○). Depth scale as in Fig. 2.

rhythm, which terminated in a complete depression in 11–24 min (Fig. 6*B*).

Addition of CO_2–HCO_3^- during anoxia

The effects of addition of CO_2–HCO_3^- during anoxia following the sequence of events described above were studied in six experiments. After reaching steady state in the nominal absence of O_2 and CO_2–HCO_3^-, superfusion with the hypoxic solution equilibrated with 5% CO_2 in N_2 (25 mM HCO_3^-) led to a rapid increase in P_{CO_2} and $[HCO_3^-]_o$, and to a partial recovery of pH_o. These effects were accompanied by reappearance of respiratory rhythm in three out of the five preparations that showed rhythmic activity at the end of the experiment in standard oxygenated saline (Fig. 6*B*). Returning to the hypoxic N_2-gassed Hepes-buffered solution again produced a fall in P_{CO_2} and pH_o, and a complete blockade of respiratory rhythm.

In a different set of experiments, neither exposure to CO_2–HCO_3^- during anoxia nor washout in the oxygenated standard solution activated respiratory rhythm in any of the six preparations where CO_2–HCO_3^- and O_2 had been removed simultaneously, which suggests an irreversible block of rhythmic activity by this experimental treatment.

Anoxia during normocapnia

In experiments of the type shown in Fig. 6*B*, it appeared that the steady-state levels of P_{CO_2} during anoxia in the CO_2–HCO_3^--containing solution were higher compared with those in the oxygenated CO_2–HCO_3^--containing solution. To test whether anoxia in the presence of CO_2–HCO_3^- indeed leads to an increase in P_{CO_2}, we changed from the standard saline gassed with 5% CO_2 in O_2 to the solution gassed with 5% CO_2 in N_2 (Fig. 7*A*). (The CO_2 content of the two gas mixtures was compared by measuring P_{CO_2} in the two solutions and they were found to be equal within ±2 mmHg.) The resulting tissue anoxia was accompanied by an increase in P_{CO_2} of 15·2 ± 8·9 mmHg and by a fall in pH_o of 0·18 ± 0·08 pH units, which was preceded in five of the seven preparations by a transient increase of 0·01 to 0·05 pH units. The simultaneous fall in $[HCO_3^-]_o$ of 4·0 ± 1·6 mM suggests that the acid end-products of anaerobic metabolism (e.g. lactic acid) titrate bicarbonate and this accounts for the increase in P_{CO_2}. Although a progressive decrease in the frequency of bursts was detected under these anoxic conditions, rhythmic activity persisted significantly longer (even up to 30 min) compared with what was seen in the CO_2–HCO_3^--free saline free of O_2. A complete suppression of respiratory rhythm was observed during the early phase of reoxygenation in five of the seven preparations (Fig. 7*A*, see also Fig. 6*B*).

Effect of anoxia on tissue profiles of P_{CO_2} and pH

In the final set of five experiments, tissue profiles of P_{CO_2} and pH_o were first determined in the oxygenated standard saline (these data are not included in the plot of Fig. 2*D*) and then again after reaching steady state in the anoxic solution gassed with 5% CO_2 in N_2 (cf. Fig. 7*A*). The measured mean values have been plotted against recording depth in Fig. 7*B*.

These data were used in the quantitative analysis (see Appendix) based on the diffusion model described in the Discussion. The results of the analysis are given in the Discussion and Appendix.

DISCUSSION

In the present study, we have used fast double- and triple-barrelled microelectrodes in combination with a conventional suction electrode to study the relationship between respiratory activity and tissue P_{CO_2}, pH_o and $[HCO_3^-]_o$ in the VRG at steady state during chemostimulation as well as upon anoxic exposure. These recently introduced microelectrodes do not suffer from interference by lactate (Voipio & Kaila, 1993), which is important when recording P_{CO_2} in a hypoxic or anoxic preparation. When considering the present results, it should be taken into account that the metabolic rate of newborn mammals is less than 20% of that in adults (Duffy, Kohle & Vannucci, 1975; Bomont, Bilger, Boyet, Vert & Nehlig, 1992; see also Ballanyi *et al.* 1996) and that the experiments were made at a reduced *in vitro* temperature of 27 °C. The results will be discussed under the following aspects: (i) relation between tissue P_{CO_2}–pH_o gradient and neuronal function; (ii) central chemosensitivity; (iii) localization of chemosensitive structures; (iv) origin of the tissue P_{CO_2}–pH_o gradient; and (v) quantitative estimation of diffusional properties of CO_2 and HCO_3^-, and metabolic rate.

Tissue P_{CO_2}–pH_o gradients and neuronal function

In neonatal rats, the neurons of the VRG, which is responsible for rhythm generation (Smith, Ellenberger, Ballanyi, Richter & Feldman, 1991), are distributed at a depth of between 300 and 600 μm below the ventral surface (Brockhaus *et al.* 1993). In this region, steady-state mean pH_o fell from 7·0 to 6·8, whereas P_{CO_2} increased from 77 to 95 mmHg in the *en bloc* preparation. These values deviate considerably from those generally considered to be physiological. However, determination of interstitial pH under *in vivo* conditions (cf. Hansen, 1985; Arita, Ichikawa, Kuwana & Kogo, 1989; cf. Chesler, 1990) revealed values that were up to 0·4 pH units lower than those of arterial blood. As recently shown for hippocampal slices, a major portion of extracellular acidosis is due to on-going CO_2 production (Voipio & Kaila, 1993; see also below). This agrees well with the *in vivo* finding that oxygen consumption results in a profound P_{O_2} gradient, ranging from about 60 mmHg in the vicinity of the arterial end of the capillaries to less than 5 mmHg close to the venous end (Grote, Zimmer & Schubert, 1981).

Under both *in vivo* and *in vitro* conditions, synchronized neuronal activity can lead to a further fall in pH_o of

0·1–0·3 pH units (Chesler, 1990; Chesler & Kaila, 1992). Recently, it has been demonstrated that tetanic stimulation of hippocampal slices leads to rises of P_{CO_2} to a maximum of 70 mmHg (Voipio & Kaila, 1993). Although it remains to be determined in detail to what extent such low pH_o and high P_{CO_2} levels affect neuronal excitability of different types of brain cells, basic functions of neonatal VRG neurons do not appear to be disturbed. In these cells, stable membrane potentials, overshooting action potentials and respiration-related synaptic potentials can be recorded for several hours *in vitro* (e.g. Ballanyi, Völker & Richter, 1994) and also during variations of the pH and/or CO_2 content of the superfusion fluid (Kawai *et al.* 1996). Furthermore, membrane properties of respiratory neurons, including respiration-related synaptic currents, were almost identical in the *en bloc* preparation and in 350–600 μm thick transverse slices, for which much flatter pH_o and P_{CO_2} profiles can be assumed (Smith *et al.* 1991). In about 50% of inspiratory neurons of the brainstem–spinal cord preparation, these characteristics remain stable even during long-term anoxia (Ballanyi *et al.* 1994), which leads to a further decrease in pH_o to values as low as 6·3 (Brockhaus *et al.* 1993; Völker *et al.* 1995). Since the extracellular anoxic acidification probably reflects an intracellular acidification, it might be hypothesized that membrane properties of neonatal respiratory neurons are similarly tolerant to intracellular acidification, as recently demonstrated for medullary dorsal vagal neurons (Trapp, Lückermann, Brooks & Ballanyi, 1996).

Central chemosensitivity

Our results on variations of the CO_2–H^+–HCO_3^- content of the superfusate confirm those of previous studies (Suzue, 1984; Harada *et al.* 1985; Okada *et al.* 1993*b*; Völker *et al.* 1995; Kawai *et al.* 1996), which established that neuronal structures reponsible for central chemosensitivity are functional in the isolated medulla. In an extension of these studies, our simultaneous measurements of CO_2, H^+ and HCO_3^- provide novel information on the interrelationship of these chemostimuli within the tissue and on their contribution to modulation of respiratory network functions.

An increase in the frequency of respiratory rhythm was observed during a comparable fall in pH_o in the VRG upon administration of a low pH solution (pH 7·0), obtained either by lowering bicarbonate or by increasing P_{CO_2}, which had opposite effects on tissue P_{CO_2}. On the contrary, depression of respiratory activity occurred after introduction of a 5% CO_2 gassed saline with elevated bicarbonate concentration (pH 7·7), which produced a considerable rise in tissue P_{CO_2} and an extracellular alkalosis. These findings suggest that a fall in tissue pH rather than a rise in P_{CO_2} is primarily responsible for stimulation of respiration as originally proposed by Loeschcke (1982).

This assumption that CO_2 *per se* might play only a minor role in central chemosensitivity is substantiated by the finding that superfusion of the CO_2–HCO_3^--free Hepes-buffered saline led to a rapid fall in tissue P_{CO_2} from above 80 mmHg to below 20 mmHg without a major effect on respiratory rhythm. The observed negligible mean increase in the frequency of respiratory rhythm in the Hepes solution can rather be attributed to the accompanying small fall in pH_o. Hence, elevation of bath pH produces a depression of rhythmic activity, whereas lowering pH causes respiratory stimulation in CO_2–HCO_3^--containing (Suzue, 1984) and also in CO_2–HCO_3^--free superfusates (Harada *et al.* 1985; Völker *et al.* 1995). In line with this, this study did not find any consistent relationship between $[HCO_3^-]_o$ and the frequency of C2 bursts.

However, it should be noted that the chemosensor response of the *in vitro* preparation is not identical to that in the intact animal. Changes in the metabolic state, as occur during hypercapnia or metabolic acidosis, do not only influence frequency, but also strength of breathing *in vivo*. In the highly reduced *in vitro* preparation, which is devoid of afferent inputs, the central nervous origin of the effects on the strength of respiratory efforts might be occluded. Nevertheless, it was demonstrated by particular integration of extracellular nerve signals that CO_2 leads to a potentiation of phrenic amplitude (Harada *et al.* 1985). A similar stimulating effect on the strength of respiratory bursts was also observed during hypercapnia in some experiments of the present study. Furthermore, hypercapnia at constant bath pH (achieved by increasing P_{CO_2} and $[HCO_3^-]$), leading to a rise in tissue P_{CO_2} without a fall in pH_o, restored rhythmic activity in some preparations, in which burst activity ceased after several hours of recording. In fresh preparations, this treatment was often coupled to a transient increase in burst frequency. Rhythmic activity reappeared also subsequent to anoxic silencing in Hepes solution after introduction of the saline gassed with 5% CO_2 and 95% N_2. These results confirm previous assumptions based on findings in the brainstem–spinal cord preparation (Harada *et al.* 1985; Völker *et al.* 1995) as well as *in vivo* (cf. Millhorn & Eldridge, 1986) that CO_2 might have a direct stimulating effect on the respiratory network.

Localization of chemosensitive structures

The work of the groups of Mitchell and Loeschcke has established that central chemosensitivity is located in neuronal structures at the ventral surface of the medulla (see Loeschcke, 1982). More recent studies, however, suggest that the stimulating effect of the localized (CO_2-induced) acidification is much smaller at the ventral surface than in deeper regions of the ventrolateral reticular formation and, in particular, in the vicinity of the VRG neurons (St John & Wang, 1977; cf. Millhorn & Eldridge, 1986; Arita *et al.* 1989). Accordingly, it was recently demonstrated in the brainstem–spinal cord preparation from neonatal rats that resting potential and respiration-related synaptic potentials change profoundly during hypercapnia (Kawai *et al.* 1996). Since, in most of these neurons, dendritic structures

projected to the ventral surface of the medulla, it could be suggested that chemosensitivity might be an intrinsic property of VRG neurons. However, in the report by Kawai *et al.* (1996), and also in a variety of different studies, it was found that tonic discharge of several types of non-respiratory neurons of the ventrolateral, and also of the dorsal, medulla is highly sensitive to variations of interstitial pH and/or CO_2 (e.g. Dean, Lawing & Millhorn, 1989; Coates, Li & Nattie, 1993; Okada *et al.* 1993*b*).

In the present study, the kinetics of the chemically induced modulation of respiratory frequency corresponded to the slow diffusion-related changes of pH_o in the VRG. For example, frequency stimulation of rhythmic activity did not follow the prominent and rapid fall in P_{CO_2} that was observed at the ventral surface after introduction of the Hepes solution. The kinetics were similar to that of the subsequent slow fall in pH_o in the region of the VRG, which was also found in the study of Völker *et al.* (1995). These results contradict other recent studies, which have suggested that the chemoresponse of the isolated respiratory network in the brainstem–spinal cord is determined by the time course of the pH changes at the ventral surface (Okada *et al.* 1993*b*; Kawai *et al.* 1996).

These examples show that the structural correlate(s) of central chemosensitivity remains yet to be determined. Future studies on the isolated medulla preparation should combine localized application of chemostimuli (e.g. Issa & Remmers, 1992) with intracellular recordings from functionally identified medullary neurons.

Origin of tissue gradients of P_{CO_2}, pH_o and $[HCO_3^-]_o$

The observed pH_o gradient is similar to that reported recently using double-barrelled H^+-sensitive microelectrodes in this preparation (Brockhaus *et al.* 1993; see also Okada *et al.* 1993*a*). There is a steep P_{O_2} gradient and an anoxic centre at tissue depths exceeding 700 μm; hence it has been assumed that the pH_o gradient originates from anaerobic production of lactic acid (Brockhaus *et al.* 1993). Maintained extracellular pH gradients have been suggested to be due to increased anaerobic metabolism also in other mammalian CNS preparations, both *in vitro* and *in vivo* (for references, see Hansen, 1985; Chesler, 1990). However, direct measurements of pH_o and P_{CO_2} have shown that the steady-state acidification in rat hippocampal slices maintained in an interface chamber is due to accumulation of extracellular CO_2 rather than a fall in $[HCO_3^-]_o$ (Voipio & Kaila, 1993), i.e. it is mainly due to a respiratory acidosis related to aerobic metabolism.

Sources and sinks of CO_2 and HCO_3^-

The substantial steady-state gradients of P_{CO_2}, pH_o and $[HCO_3^-]_o$ observed in the present study can be accounted for by a model that is qualitatively described by Fig. 8. An H^+ load generated by cellular metabolism may be buffered by the CO_2–HCO_3^- buffer system within cells, as well as in the interstitial space. At steady state, these reactions are in balance with active transport of acid equivalents across cell membranes. This creates a source of CO_2 and a sink of HCO_3^- with a 1:1 stochiometry in the tissue. The hydration–dehydration reaction of CO_2–HCO_3^- is rapid only when catalysed by the enzyme carbonic anhydrase (e.g. Maren, 1984). The evidence obtained in this study suggesting the presence of extracellular carbonic anhydrase activity indicates that significant net dehydration may occur also in the interstitial space of the present preparation.

The finding that P_{CO_2} in the VRG decreased from about 90 mmHg to below 20 mmHg upon superfusion of the CO_2–HCO_3^--free solution, and further to below 1 mmHg following removal of O_2, indicates that titration of bicarbonate by protons is a significant source of CO_2 in addition to its direct production by aerobic metabolism. This conclusion is supported also by the rapid decrease in $[HCO_3^-]_o$ with increasing tissue depths under control conditions, which is in line with consumption of bicarbonate at a high rate in buffering of an H^+ load within the tissue.

A rough estimate of the direct CO_2 production by aerobic metabolism is given by the difference between tissue P_{CO_2} levels during anoxia and in the oxygenated Hepes-buffered solution. However, it is not correct to assume that a given rate of aerobic CO_2 production would make a quantitatively similar contribution to the tissue gradient of P_{CO_2} under all conditions. In the nominal absence of CO_2–HCO_3^-, the gradients of tissue P_{CO_2} and $[HCO_3^-]_o$ are both oriented so that they give rise to corresponding net fluxes from the tissue to the bath. Therefore, the diffusion of CO_2 occurs partially via the flux of HCO_3^-, which flattens the P_{CO_2} profile. Such facilitation of CO_2 transfer does not occur under control conditions, since the opposite orientation of the $[HCO_3^-]_o$ gradient results in net diffusion of HCO_3^- into the tissue. It is therefore evident that the contribution of aerobic metabolism (at a given rate) to the elevated P_{CO_2} in the VRG is larger under control conditions than in the nominal absence of CO_2–HCO_3^-.

Exposure to a solution devoid of O_2 causes anoxia of the entire preparation and leads, by increased anaerobic glycolysis, to potentiation of metabolic acid production (Brockhaus *et al.* 1993; Völker *et al.* 1995; Ballanyi *et al.* 1996), which is seen as a fall in pH_o. The resulting stimulation of HCO_3^- titration accounts for the observed rise in P_{CO_2} and the fall in $[HCO_3^-]_o$. The depletion of CO_2 from the preparation during anoxia in the CO_2–HCO_3^--free solution rules out any significant role of decarboxylation reactions as a source of CO_2, at least under these conditions. This also holds true for carbamate compounds, although they may have an effect during changes in P_{CO_2}. Therefore, titration of HCO_3^- is the only mechanism generating CO_2 under anoxic conditions within the tissue.

It may be concluded that the sources and sinks of CO_2 and HCO_3^- consist of operation of the CO_2–HCO_3^- buffer system and direct production of CO_2 by aerobic metabolism.

The relative contributions of individual mechanisms are likely to vary under different experimental conditions and at different tissue depths.

Pathways of CO_2 and HCO_3^- through the tissue

Being electrically neutral, CO_2 molecules permeate phospholipid membranes easily; their pathway has been drawn in Fig. 8 as a straight line through the tissue. Two mechanisms may play a role within the various compartments of the tissue: the diffusion of CO_2 may be either facilitated (cf. Longmuir, Forster & Woo, 1966; Gros, Moll, Hoppe & Gros, 1976) or retarded by macromolecular structures (e.g. Gros & Moll, 1971), or both. On the other hand, membranes form a diffusion barrier to bicarbonate ions, limiting their free diffusion through the tissue to the tortuous interstitial space.

While translocating acid equivalents from the preparation to the bath, the CO_2–HCO_3^- shuttle gives rise to a net movement of negative charge into the tissue (Fig. 8). It is reasonable to assume that electroneutrality is maintained, at least partly, by the flux of lactate anions (A^-) from the tissue.

pH_o gradient

Although the diffusion coefficient or the limiting equivalent conductivity of H^+ ions is high compared with those of other cations (Robinson & Stokes, 1959), net acid fluxes carried by free protons are bound to be negligible due to their very low concentration at physiological pH levels. However, the diffusion of protonated and non-protonated buffer species down their concentration gradients, caused by a pH gradient, can facilitate the diffusion of protons by orders of magnitude. Such an effect has been demonstrated in concentrated solutions of phosphate (Gros *et al.* 1976). In the present study, omitting the small amount of NaH_2PO_4 (1·2 mM) in the standard saline did not have a notable effect on pH_o. Therefore, the mechanism responsible for clearing of the acid generated by cellular metabolism consists of continuous fluxes of bicarbonate into, and CO_2 out of, the preparation as illustrated in Fig. 8, and the resulting pH_o gradient depends on the ability of CO_2 and HCO_3^- to diffuse through the tissue. If present in sufficiently high concentrations, shuttles of protonated and non-protonated forms of other buffers (e.g. Hepes) may contribute as shown in Fig. 8.

The finding that aerobic production of CO_2 is not the main cause of the low pH_o in the present preparation appears to contradict the result cited above, which was obtained with the same microelectrode technique in rat hippocampal slices. However, this is not the case since the oxygen supply of a 400 μm thick slice preparation maintained in an interface chamber (cf. Voipio & Kaila, 1993) is far better than that of the superfused brainstem having a diameter of more than 2000 μm.

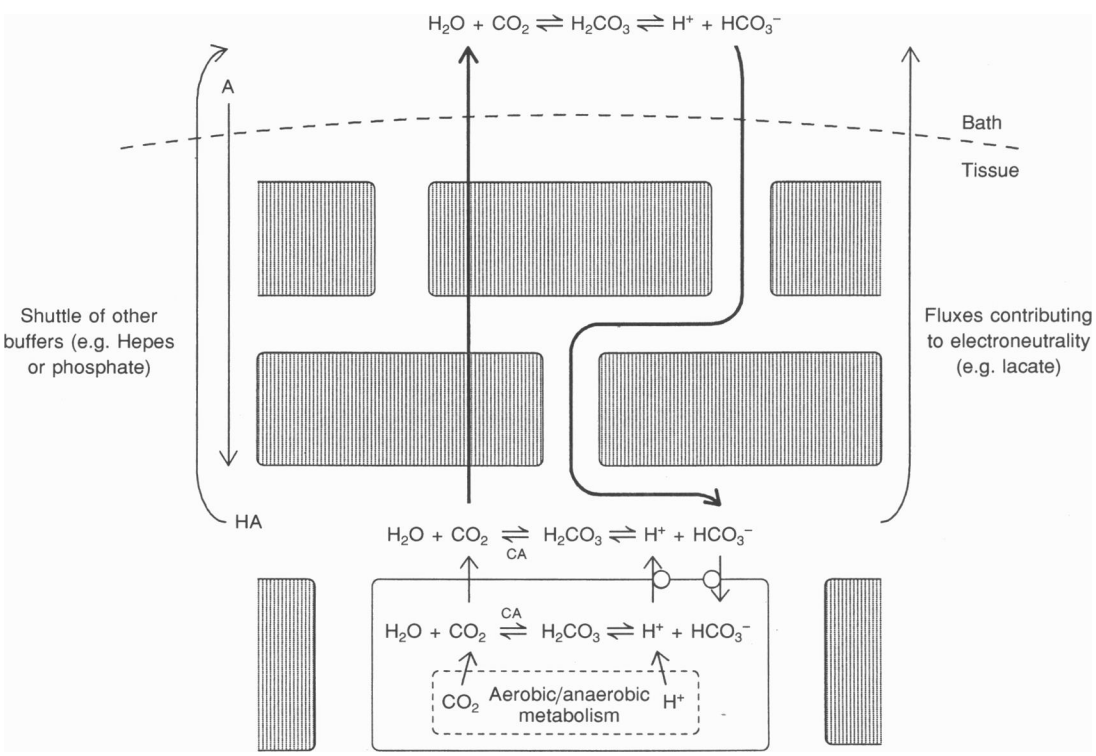

Figure 8. Diffusion of acid equivalents in brain tissue

A schematic representation of the proposed model showing the mechanisms involved in diffusion of acid equivalents in brain tissue. Rectangles represent single cells; long arrows indicate diffusion fluxes; CA, carbonic anhydrase; HA and A, protonated and non-protonated forms, respectively, of a non-CO_2–HCO_3^- buffer. For details, see text.

Choice of saline for an *in vitro* preparation

At a more general level, it can be concluded from the above discussion that, in addition to rapid buffering, the availability of easily diffusing buffer molecules is essential in reducing pH_o gradients in superfused CNS preparations *in vitro*. In light of the present results, increasing the bicarbonate content of the standard solution (e.g. by 5–10 mM) and reducing the CO_2 content of the gas mixture (e.g. to 3% CO_2 in O_2) would result in more physiological conditions within a preparation like the *in vitro* brainstem of neonatal rats. This can be taken as an area for future work (see also Okada *et al.* 1993*a*, *b*; Kawai *et al.* 1996).

Results obtained using diffusion equations

A quantitative analysis of the diffusion of CO_2 and HCO_3^- and their anoxia profiles is given in the Appendix and it yields three interesting results. First, the diffusion coefficient of CO_2 at tissue level in the neonatal rat brainstem does not differ from that in the saline. Second, the HCO_3^- flux related to a given concentration gradient is four to five times larger in water than in the present preparation under anoxic conditions. This factor is given by λ^2/α (where λ denotes tortuosity and α denotes extracellular space volume fraction) and its relatively small value compared with results from mature rat CNS (e.g. about twelve in the paper by Nicholson & Phillips, 1981; note that $\lambda^2/\alpha = 1$ in water) is in agreement with the relative reduction in extracellular space during maturation of the CNS (Lehmenkühler, Sykova, Svoboda, Zilles & Nicholson, 1993; see also Nicholson & Rice, 1986). Third, the metabolic rate of anoxic tissue was calculated from the concentration profiles of CO_2 and HCO_3^- as the rate of acid production, and the two mean estimates obtained were 1·13 and 1·08 mequiv l^{-1} min^{-1}, respectively.

In the *in vivo* adult rat spinal cord grey matter, ischaemia induces a pronounced decrease in the extracellular space volume fraction, as well as an increase in tortuosity (Sykova, Svoboda, Polak & Chvatal, 1994). On the other hand, in the somatosensory neocortex of 2- to 3-day-old rats, λ^2/α is about six under normoxic conditions (Lehmenkühler *et al.* 1993). Compared with these results, the mean estimates of λ^2/α (4·75 and 4·1 or 4·5; see Appendix) obtained under anoxic conditions in the present study can be taken as further evidence of the excellent anoxia tolerance of the *in vitro* neonatal brainstem preparation (see Ballanyi *et al.* 1994). However, the obtained λ^2/α values remain to be confirmed in future work by using the well-established tetramethyl ammonium (TMA) injection method (Nicholson & Phillips, 1981; see also Nicholson & Rice, 1986).

From the present data, it is not possible to calculate a reliable estimate of $\alpha(D_{HCO_3^-}/\lambda^2)$ under aerobic conditions (where D is diffusion coefficient, see below). However, if this was done using the TMA injection method, the data on $[HCO_3^-]_o$ and tissue P_{CO_2} as a function of tissue depth under control conditions could be used to obtain estimates of the rates of aerobic and anaerobic metabolism, as well as of the flux and the partial pressure of oxygen. Interestingly, preliminary calculations based on the present data predict a P_{O_2} profile with a shape similar to that measured with O_2 microelectrodes (Brockhaus *et al.* 1993).

APPENDIX

Diffusion in isotropic media is described by Fick's Laws (Crank, 1956). Introducing the concepts of volume fraction (α), tortuosity (λ) and volume averaging makes it possible to modify these equations for diffusion of impermeable substances along the extracellular space in brain tissue (Nicholson & Phillips, 1981).

Quantitative analysis of the present results starts from the observation that, at steady state under anoxic conditions in the CO_2–HCO_3^--containing saline (5% CO_2 in N_2), all CO_2 that is generated in the tissue comes from titration of HCO_3^-. Therefore, under these conditions, the source density of CO_2 and the sink density of HCO_3^- are equal throughout the whole preparation, and at each depth within the tissue the volume-averaged flux of HCO_3^- ($\langle \bar{J}_{HCO_3^-} \rangle$) and the flux of CO_2 ($\bar{J}_{CO_2}$) are equal in magnitude but have opposite directions (see Fig. 8):

$$-\langle \bar{J}_{HCO_3^-} \rangle = \bar{J}_{CO_2}, \quad \text{(A1)}$$

or

$$\alpha(D_{HCO_3^-}/\lambda^2)\nabla[HCO_3^-]_o = -D_{CO_2,tissue} S_{CO_2} \nabla P_{CO_2}, \quad \text{(A2)}$$

where $D_{HCO_3^-}$ and $D_{HCO_3^-}/\lambda^2$ are the free and apparent diffusion coefficients of HCO_3^-, S_{CO_2} is the solubility of CO_2 in water (0·04 mmol l^{-1} $mmHg^{-1}$) and $S_{CO_2}\nabla P_{CO_2}$ gives the concentration gradient of CO_2. Since CO_2 permeates membranes easily, its flux is given by the unmodified Fick's Law and the possible facilitating and/or retarding mechanisms (see Discussion) are incorporated into the effective diffusion coefficient of CO_2 in the tissue ($D_{CO_2,tissue}$). The factor of λ^2/α compares water with tissue as media for a macroscopic flux of bicarbonate; therefore $\alpha D_{HCO_3^-}/\lambda^2$ is also an intuitively meaningful parameter.

It is obvious that the flux of CO_2 can change only smoothly as a function of tissue depth and does not change at the tissue surface when entering the unstirred layer surrounding the preparation. Somewhat surprisingly, there was no detectable shift in the slope of the P_{CO_2} profile at the tissue surface, which indicates that $D_{CO_2,tissue}$ equals the diffusion coefficient of CO_2 in saline ($D_{CO_2,saline}$). This means that neither facilitating nor retarding mechanisms play a significant role in CO_2 diffusion in the neonatal rat brainstem, or that these mechanisms cancel the effect of each other. In the light of published data (see Ratcliff & Holdcroft, 1963; Gros & Moll, 1971) $D_{CO_2,saline}$ is $1{\cdot}84 \times 10^{-5}$ cm^2 s^{-1} under the experimental conditions of this study.

A similar approach is not necessarily valid for HCO_3^- because there is no carbonic anhydrase in the superfusion solution. Instead, using eqn (A2) and local slopes of individual anoxia profiles at depths from tissue surface to below the VRG gives an estimate of $\alpha(D_{HCO_3^-}/\lambda^2)$ of

$0{\cdot}23 \times 10^{-5} \pm 0{\cdot}11 \times 10^{-5}$ cm^2 s^{-1} (mean ± S.D., $n = 5$). Taking into account the effect of ionic strength on $D_{HCO_3^-}$ (see Appendix in Gros & Moll, 1974), the limiting equivalent conductivity of bicarbonate (44·5 S cm^2 equiv^{-1}; Robinson & Stokes, 1959) yields $D_{HCO_3^-} = 0{\cdot}88 \times 10^{-5}$ cm^2 s^{-1} in saline solutions used in the present study. The data therefore give $\lambda^2/\alpha = 4{\cdot}75 \pm 2{\cdot}3$ for anoxic tissue. This means that the HCO_3^- flux related to a given concentration gradient is about four to five times larger in water than in the present preparation under anoxic conditions.

Fick's Second Law can be written for CO_2, and in its modified form for HCO_3^-:

$$S_{CO_2}(\partial/\partial t)P_{CO_2} = D_{CO_2,tissue}S_{CO_2}\nabla^2 P_{CO_2} + q_{CO_2}, \quad \text{(A3)}$$

$$\alpha(\partial/\partial t)[HCO_3^-]_o = \alpha(D_{HCO_3^-}/\lambda^2)\nabla^2[HCO_3^-]_o + \langle q_{HCO_3^-}\rangle, \quad \text{(A4)}$$

where q_{CO_2} is the source density of CO_2 and $\langle q_{HCO_3^-}\rangle$ is the volume average of the extracellular source density of HCO_3^- related to buffering in the extracellular space and active transport of bicarbonate across cell membranes, i.e. at steady state it is the net effect of buffering in both extracellular and intracellular compartments. These equations can be written for radial diffusion in spherical polar co-ordinates by simply replacing ∇^2 by:

$$\partial^2/\partial r^2 + (2/r)(\partial/\partial r),$$

where r is the distance from the centre of the sphere, and for radial diffusion in cylindrical co-ordinates by replacing ∇^2 by:

$$\partial^2/\partial r^2 + (1/r)(\partial/\partial r).$$

At steady state, the time derivatives in eqns (A3) and (A4) become zero and, since the sink density $-\langle q_{HCO_3^-}\rangle$ equals q_{CO_2} during anoxia, we get:

$$\lambda^2/\alpha = -(D_{HCO_3^-}\nabla^2[HCO_3^-]_o)/(D_{CO_2,tissue}S_{CO_2}\nabla^2 P_{CO_2}). \quad \text{(A5)}$$

This equation and the curvatures of the anoxia profiles give another estimate of λ^2/α of $4{\cdot}1 \pm 1{\cdot}8$ ($n = 5$) when considering radial diffusion in cylindrical co-ordinates, or $4{\cdot}5 \pm 2{\cdot}9$ for the case of one-dimensional diffusion in rectangular co-ordinates, both of which are in good agreement with the result obtained above using eqn (A2). In future work, it will be interesting to compare these estimates with those obtainable by the TMA injection method (Nicholson & Phillips, 1981; see also Nicholson & Rice, 1986).

Equations (A3) and (A4) and the anoxia profiles can also be used to calculate estimates of $-\langle q_{HCO_3^-}\rangle$ and q_{CO_2}, i.e. the steady-state rate of acid production by the preparation during anoxia. The values obtained are almost equal, namely $q_{CO_2} = 1{\cdot}13 \pm 0{\cdot}57$ mequiv l^{-1} min^{-1} and, using $\alpha(D_{HCO_3^-}/\lambda^2) = 0{\cdot}23 \times 10^{-5}$ cm^2 s^{-1} in eqn (A4), $-\langle q_{HCO_3^-}\rangle = 1{\cdot}08 \pm 0{\cdot}41$ mequiv l^{-1} min^{-1}.

ARITA, H., ICHIKAWA, K., KUWANA, S. & KOGO, N. (1989). Possible locations of pH-dependent central chemoreceptors: intramedullary regions with acidic shift of extracellular fluid pH during hypercapnia. *Brain Research* **485**, 285–293.

BALLANYI, K., VÖLKER, A. & RICHTER, D. W. (1994). Anoxia induced functional inactivation of neonatal respiratory neurons *in vitro*. *NeuroReport* **6**, 165–168.

BALLANYI, K., VÖLKER, A. & RICHTER, D. W. (1996). Functional relevance of anaerobic metabolism in the isolated respiratory network of newborn rats. *Pflügers Archiv* **432**, 741–748.

BOMONT, L., BILGER, A., BOYET, S., VERT, P. & NEHLIG, A. (1992). Acute hypoxia induces specific changes in local cerebral glucose utilization at different postnatal ages in the rat. *Developmental Brain Research* **66**, 33–45.

BROCKHAUS, J., BALLANYI, K., SMITH J. C. & RICHTER, D. W. (1993). Microenvironment of respiratory neurons in the *in vitro* brainstem–spinal cord of neonatal rats. *Journal of Physiology* **462**, 421–445.

CHESLER, M. (1990). The regulation and modulation of pH in the nervous system. *Progress in Neurobiology* **34**, 401–427.

CHESLER, M. & KAILA, K. (1992). Modulation of pH by neuronal activity. *Trends in Neurosciences* **15**, 396–402.

COATES, E. L., LI, A. & NATTIE, E. E. (1993). Widespread sites of brain stem ventilatory chemoreceptors. *Journal of Applied Physiology* **75**, 5–14.

CRANK, J. (1956). *The Mathematics of Diffusion*. Clarendon Press, Oxford.

DEAN, J. B., LAWING, W. L. & MILLHORN, D. E. (1989). CO_2 decreases membrane conductance and depolarizes neurons in the nucleus tractus solitarii. *Experimental Brain Research* **76**, 656–661.

DUFFY, T. E., KOHLE, S. J. & VANNUCCI, R. C. (1975). Carbohydrate and energy metabolism in perinatal rat brain: relation to survival in anoxia. *Journal of Neurochemistry* **24**, 271–276.

GROS, G. & MOLL, W. (1971). The diffusion of carbon dioxide in erythrocytes and hemoglobin solutions. *Pflügers Archiv* **324**, 249–266.

GROS, G. & MOLL, W. (1974). Facilitated diffusion of CO_2 across albumin solutions. *Journal of General Physiology* **64**, 356–371.

GROS, G., MOLL, W., HOPPE, H. & GROS, H. (1976). Proton transport by phosphate diffusion – a mechanism of facilitated CO_2 transfer. *Journal of General Physiology* **67**, 773–790.

GROTE, J., ZIMMER, K. & SCHUBERT, R. (1981). Effects of severe arterial hypocapnia on regional blood flow regulation in the brain cortex of cats. *Pflügers Archiv* **391**, 195–199.

GUTKNECHT, J. & TOSTESON, D. C. (1973). Diffusion of weak acids across lipid bilayer membranes: effects of chemical reactions in the unstirred layers. *Science* **182**, 1258–1261.

HANSEN, A. J. (1985). Effect of anoxia on ion distribution in the brain. *Physiological Reviews* **65**, 101–148.

HARADA, Y., KUNO, M. & WANG, Y. Z. (1985). Differential effects of carbon dioxide and pH on central chemoreceptors in the rat *in vitro*. *Journal of Physiology* **368**, 679–693.

ISSA, F. G. & REMMERS, J. E. (1992). Identification of a subsurface area in the ventral medulla sensitive to local changes in P_{CO_2}. *Journal of Applied Physiology* **72**, 439–446.

KAILA, K., PAALASMAA, P., TAIRA, T. & VOIPIO, J. (1992). pH transients due to monosynaptic activation of $GABA_A$ receptors in rat hippocampal slices. *NeuroReport* **3**, 105–108.

KAWAI, A., BALLANTYNE, D., MÜCKENHOFF, K. & SCHEID, P. (1996). Chemosensitive medullary neurones in the brainstem–spinal cord preparation of the neonatal rat. *Journal of Physiology* **492**, 277–292.

KUWANA, S., BALLANYI, K., MORAWIETZ, G., VÖLKER, A., VOIPIO, J. & RICHTER, D. W. (1993). Chemosensitivity of the respiratory network of neonatal and mature rats. *XXXII Congress of the International Union of Physiological Sciences* **1141**, 26P.

LEHMENKÜHLER, A., SYKOVA, E., SVOBODA, J., ZILLES, K. & NICHOLSON, C. (1993). Extracellular space parameters in the rat neocortex and subcortical white matter during postnatal development determined by diffusion analysis. *Neuroscience* **55**, 339–351.

LOESCHCKE, H. H. (1982). Central chemosensitivity and the reaction theory. *Journal of Physiology* **332**, 1–24.

LONGMUIR, I. S., FORSTER, R. E. & WOO, C. Y. (1966). Diffusion of carbon dioxide through thin layers of solution. *Nature* **209**, 393.

MAREN, T. H. (1984). The general physiology of reactions catalyzed by carbonic anhydrase and their inhibition by sulfonamides. *Annals of the New York Academy of Sciences* **429**, 568–579.

MILLHORN, D. E. & ELDRIDGE, F. L. (1986). Role of ventrolateral medulla in regulation of respiratory and cardiovascular systems. *Journal of Applied Physiology* **61**, 1249–1263.

NICHOLSON, C. & PHILLIPS, J. M. (1981). Ion diffusion modified by tortuosity and volume fraction in the extracellular microenvironment of the rat cerebellum. *Journal of Physiology* **321**, 225–257.

NICHOLSON, C. & RICE, M. E. (1986). The migration of substances in the neuronal microenvironment. *Annals of the New York Academy of Sciences* **481**, 55–68.

OKADA, Y., MÜCKENHOFF, K., HOLTERMANN, G., ACKER, H. & SCHEID, P. (1993*a*). Depth profiles of pH and pO_2 in the isolated brainstem–spinal cord of the neonatal rat. *Respiration Physiology* **93**, 315–326.

OKADA, Y., MÜCKENHOFF, K. & SCHEID, P. (1993*b*). Hypercapnia and medullary neurons in the isolated brainstem–spinal cord of the rat. *Respiration Physiology* **93**, 327–336.

RATCLIFF, G. A. & HOLDCROFT, J. G. (1963). Diffusivities of gases in aqueous electrolyte solutions. *Transactions of the Institution of Chemical Engineers* **41**, 315–319.

ROBINSON, R. A. & STOKES, R. H. (1959). *Electrolyte Solutions*, p. 463. Butterworths, London.

ST JOHN, W. M. & WANG, S. C. (1977). Responses of medullary respiratory neurons to hypercapnia and isocapnic hypoxia. *Journal of Applied Physiology* **43**, 812–821.

SMITH, J. C., ELLENBERGER, H. H., BALLANYI, K., RICHTER, D. W. & FELDMAN, J. L. (1991). Pre-Bötzinger complex: a brainstem region that may generate respiratory rhythm in mammals. *Science* **254**, 726–729.

SUZUE, T. (1984). Respiratory rhythm generation in the *in vitro* brainstem–spinal cord preparation of the neonatal rat. *Journal of Physiology* **354**, 173–183.

SYKOVA, E., SVOBODA, J., POLAK, J. & CHVATAL, A. (1994). Extracellular volume fraction and diffusion characteristics during progressive ischemia and terminal anoxia in the spinal cord of the rat. *Journal of Cerebral Blood Flow and Metabolism* **14**, 301–311.

TRAPP, S., LÜCKERMANN, M., BROOKS, P. S. & BALLANYI, K. (1996). Acidosis of dorsal vagal neurons *in situ* during spontaneous and evoked activity. *Journal of Physiology* **496**, 695–710.

VOIPIO, J. & BALLANYI, K. (1993). Direct measurements of tissue pCO_2 in the *in vitro* brainstem–spinal cord of neonatal rats. *Proceedings of 21st Göttingen Neurobiology Conference*, ed. ELSNER, N. & HEISENBERG, M., p 331. Thieme Verlag, Stuttgart, New York.

VOIPIO, J. & KAILA, K. (1993). Interstitial P_{CO_2} and pH in rat hippocampal slices measured by means of a novel fast CO_2/H^+-sensitive microelectrode based on a PVC-gelled membrane. *Pflügers Archiv* **423**, 193–201.

VOIPIO, J., PAALASMAA, P., TAIRA, T. & KAILA, K. (1995). Pharmacological characterization of extracellular pH transients evoked by selective synaptic and exogenous activation of AMPA, NMDA, and $GABA_A$ receptors in the rat hippocampal slice. *Journal of Neurophysiology* **74**, 633–642.

VOIPIO, J., PASTERNACK, M. & MACLEOD, K. (1994). Ion-sensitive microelectrodes. In *Microelectrode Techniques – The Plymouth Workshop Handbook*, 2nd edn, ed. OGDEN, D., pp. 275–316. The Company of Biologists Ltd, Cambridge.

VÖLKER, A., BALLANYI, K. & RICHTER, D. W. (1995). Anoxic disturbance of the isolated respiratory network of neonatal rats. *Experimental Brain Research* **103**, 9–19.

Acknowledgements

This work was supported by the Deutsche Forschungsgemeinschaft and the Academy of Finland.

Authors' email addresses

J. Voipio: juha.voipio@helsinki.fi

K. Ballanyi: kb@neuro-physiol.med.uni-goettingen.de

Received 27 June 1996; accepted 14 November 1996.